PNAS
www.pnas.org

Supplementary Information for

Interfacial fluid transport is a key to hydrogel bioadhesion

Raphaël Michel, Léna Poirier, Quentin van Poelvoorde, Josette Legagneux, Mathieu Manassero and Laurent Corté

Laurent Corté
Email: laurent.corte@mines-paristech.fr
Raphaël Michel
Email: r.michel3@hotmail.fr

This PDF file includes:

Supplementary Information text (Materials and Methods)
Figs. S1 to S16
Captions for movies S1 to S8
References for SI reference citations

Other supplementary materials for this manuscript include the following:

Movies S1 to S8

www.pnas.org/cgi/doi/10.1073/pnas.1813208115

SI Materials and Methods

1. Materials

1.1- Materials.

The chemicals used in this work were used as purchased without further purification. Sodium Chloride (≥ 99%), Ethanol (≥ 99.8%), Pentaerythritol tetrakis(3-mercaptopropionate) (QT, ≥ 95%), Poly(ethylene glycol) diacrylate (PEGDA, M_n = 700 kg/mol) and Fluorescein sodium salt were purchased from Sigma-Aldrich. Triethylamine (TEA, ≥ 99%) and 1,6-hexanedithiol (HT, 97%) were purchased from Alfa Aesar. The peptide GCGYGRGDSPG was purchased from GenScript. Polyethylene thin films were cut from polyethylene sample bags purchased from VWR. Commercial pressure sensitive adhesives (PSA) in the form of self-stick notes were purchased from Office Depot Europe. Oxidized regenerated cellulose mesh (Surgicel®) was purchased from Ethicon. Sterile gauze pads (Medicomp® 10x10 cm) were purchased from Hartmann.

1.2- *Ex vivo* liver tissues.

Porcine liver tissues were obtained from two different sources. Freshly dissected livers were harvested from freshly killed 3-month old pigs (*Sus scrofa domesticus*, approx. 25 kg) at the Ecole de Chirurgie du Fer-à-Moulin (AP-HP) (7 Rue du Fer À Moulin, 75005, Paris, France) in accordance with the principles of animal care. Whole livers were transported in a cooler and were stored at 4°C in physiological serum. They were used between 2 and 30 hours following their harvesting. Drained pig livers with traceability certificate were purchased from the butcher's shop 'Aux Fleurons de la Viande' (59 rue Monge, 75005 Paris, France). Drained livers were transported in a cooler and stored at 4°C. They were used during the 3 days following their purchase (18-76h after harvesting). Tissues were not stored in the freezer at any time as this is

known to alter their integrity (1). During those storage times, no significant evolution of the adhesive properties was observed.

2. PEG hydrogel fabrication and characterization

2.1- Pure PEG hydrogel fabrication.

The PEG hydrogel films were prepared by chemically crosslinking poly(ethylene glycol)diacrylate (PEGDA) with a mixture of hexanedithiol (HT) and pentaerythritol tetrakis(3-mercaptopropionate) (QT) in 15 wt.% ethanol and using tryethylamine (TEA) as catalyst. The monomers were combined in a ratio (PEGDA/HT/QT: 24/22/1) such that acrylate groups and thiol groups were present in equal quantities. The concentration of TEA was adjusted as to account for 1 mol% of all thiol groups present.

PEGDA, HT and the corresponding fraction of TEA were first mixed at 21°C and left to react under stirring (150 rpm) until conversion of 90% of acrylate groups is achieved (as confirmed by infrared spectroscopy). QT, ethanol, and the remaining TEA were then added to the mixture and further stirred at the same temperature for 10 minutes. The mixture was injected in rectangular glass molds of 100 mm × 80 mm × 1.1 mm. The molds were sealed and stored for 5 days at room temperature (20±2°C). After removal from the molds, the so-obtained hydrogel films were vacuum-dried until complete evaporation of the ethanol and triethylamine. They were then thoroughly washed by immersion (> 3h) in ultrapure water to eliminate the extractible soluble fraction (< 0.1 wt.%). The washed hydrogel membranes were subsequently dried in an oven at 60°C until complete water evaporation. The resulting dry PEG films had a thickness of 1 ± 0.03 mm.

2.2- RGD modified PEG hydrogel fabrication.

PEG hydrogel films were modified to contain an RGD peptide sequence allowing specific adhesion to cell membrane receptors. For that, the synthesis of the pure PEG hydrogel was slightly modified to graft GCGYGRGDSPG peptides to the PEG network in a similar manner as in reference (2, 3). Grafting was obtained through a Michael addition between the thiol function of cystein (C) and the acrylate end functions of PEGDA. Formulation was designed so as to reach a final peptide concentration of 80 pmol/µL in the gel, which has been shown to be well within the range (0.1-1000 pmol/µL) for which an effect on cell adhesion is observed (2-4).

Peptides were grafted to PEGDA by dissolving 1 mg of GCGYGRGDSPG into 0.5 mL of an aqueous solution containing PEGDA (6.8 g/L) and TEA (1.0 g/L). A large excess in acrylate functions was chosen here (acrylate/thiol : 10/1 molar) to favor the formation of PEGDA chains with only one grafted peptide. The solution was left to react under stirring (250 rpm) at 20 ± 1°C for 16 hours. The successful grafting of GCGYGRGDSPG on PEGDA was confirmed by IR spectroscopy by following the disappearance of the acrylate peak using a similar protocol as in reference (5).

The so-obtained RGD modified PEGDA solution was added to the mixture of PEGDA, HT and TEA described in section 2.1 and left under stirring (150 rpm) at 21°C for 15 minutes. QT, ethanol, and the remaining TEA in the same proportions as in section 2.1 were then added to the mixture and further stirred at the same temperature for 2 minutes. The mixture was then injected in rectangular glass molds of 100 mm × 80 mm × 1.1 mm. The molds were sealed and stored for 4 days at 20±2°C. After removal from the molds, the hydrogel films were vacuum-dried until complete evaporation of the water, ethanol and triethylamine. They were then thoroughly washed by immersion (> 3h) in ultrapure water to eliminate the extractible soluble fraction (≤ 0.3 wt.%). The washed hydrogel membranes were subsequently dried in an oven at

60°C until complete water evaporation. The resulting dry films had a thickness of 1 ± 0.03 mm and an equilibrium swelling ratio identical to that of the pure PEG film (see **Fig. S2**).

2.3- Mechanical characterization.

The mechanical characterization and measurement of Young's modulus, *E*, of the PEG films were performed on a tensile test apparatus (All Around, Zwick) equipped with a 10 N load cell and a videoextensometer. Rectangular stripes were cut from dry PEG films with dimensions 50 mm × 10 mm × 1 mm. Samples were stretched to a maximum strain of 3 % and unstretched at room temperature at a speed of 1 mm. s^{-1} (strain rate of approx. 0.04 s^{-1}). Samples exhibited a perfectly elastic behavior with no noticeable residual deformation and negligible hysteresis (see **Fig. S11**). The Young's modulus was found equal to 1.07 ± 0.09 MPa for dry PEG films (Q = 1) and 0.5 ± 0.09 MPa for hydrogel PEG films swollen to equilibrium (Q_{eq} = 2).

3. Adhesion measurements

3.1- Preparation of liver substrates

Rectangular liver samples were cut from liver lobes with typical dimensions 120 mm × 30 mm × 10 mm using a sharp knife. They were then glued on the bottom face onto a flat holder using cyanocrylate glue. Either the capsule surface or the parenchyma surface was exposed to air on the top face.

In the case of peeling on the liver capsule, the liver samples were immersed twice for 30 seconds in physiological serum. This gentle washing removed traces of coagulated blood that may influence adhesive properties. In the case of peeling on the liver parenchyma, the liver samples were used as prepared for freshly explanted and drained livers. For rehydrated livers, samples from drained livers were immersed for various amounts of time in physiological serum prior to mounting on the sample holder.

3.2- Preparation and deposition of peeling ribbons

Hydrogel or polyethylene ribbons were deposited at the surface of liver samples. In the case of peeling on the liver capsule, ribbons were first put in contact with the tissues exactly 3 minutes after the end of the second tissue immersion in physiological serum. In the case of peeling on the liver parenchyma, this deposition took place 10 ± 2 min after the tissues were removed from storage at 4°C. For rehydrated livers, ribbon deposition occurred 10 ± 2 min after the end of the tissue swelling period in physiological serum.

Contact pressure was applied during the first 1 minute of contact by pressing repeatedly with one finger over the whole contact area and measuring the force with a scale. A maximum force of 6 N was applied at each finger pressure. The ribbons were then left in contact for a given contact time prior to peeling. During this contact time, the whole systems were wrapped in thin plastic sheets so as to prevent evaporation.

For experiments with varying initial hydrogel swelling, PEG ribbons were swollen at the desired ratio Q and left to equilibrate for a minimum of 4 hours to ensure a homogeneous water content throughout the gel thickness.

3.3- Peeling experiments.

Peeling experiments were performed on tensile test apparatus (All Around, Zwick) equipped with a 90° peeling device and a 10 N load cell. All peeling experiments were performed at 1 mm/s. The system was synchronized with video cameras to record side and front views of the peeling zone. For each experiment, ribbons were weighed just before and just after peeling to determine the amount of fluid absorbed by the hydrogel during contact.

3.4- Peeling data analysis

3.4.1 Correction and normalization of peeling force

For experiments with the lowest level of adhesion, the weight of the ribbon lifted during peeling could not be neglected (see **Fig. S12**). As a result, the peeling force was systematically corrected by subtracting the weight of the lifted ribbon as follows:

$$F = F^* - \rho d \tag{S1}$$

where F is the corrected force, F^* the raw peeling force as measured by the cell force, d the displacement and ρ the linear mass of the ribbon. In all the work, the corrected peeling force normalized by the width of the peeled ribbon, F/w, is used.

3.4.2 Calculation of adhesion energy

Adhesion energy, G, was obtained from peeling measurements using the model for elastic peeling by Kendall (6). For that, we verified that the bending contributions can be neglected (7). In each experiment, a steady state was reached with a constant peeling profile and a peeling angle equal to 90° after the first 10 to 20 millimeters of displacement (see **Fig. S13**). An average peeling force was measured by averaging the value of the corrected force during this steady state regime. The liver sections occasionally exhibited large defects such as gaping blood vessels or capsule cavities which locally causes a loss of adhesion. These areas were systematically identified and excluded from the calculation of the average peeling force.

For 90° peeling angle, the adhesion energy of one peeling experiment is then given by:

$$G = \frac{F}{w} - \frac{F}{2w}\left(\frac{F}{Ewt}\right) \tag{S2}$$

where F is the average corrected force during steady state peeling, w, t and E the width, thickness and Young's modulus of the peeled ribbon, respectively. For all the experiments of this study, the stress applied F/wt was much smaller than the elastic modulus E which is in the range 0.5-1 MPa.

Therefore, the contribution of the second elastic term $\frac{F}{2w}\left(\frac{F}{Ewt}\right)$ can be neglected and adhesion energy is simply given by $G = F/w$.

3.4.3 Determination of lubricated and adhesive regimes

The lubricated or adhesive nature of peeling was determined for each experiment by examining the front views during peeling. If a liquid meniscus was observed at the detachment front between the gel and the tissue for more than half of the peeling length, the regime was considered "lubricated" (represented by empty symbols on the adhesion energy graphs). In this case, no tissue deformation was noticed (as being non-existent or as being contained below the level of liquid). On the contrary, if no interstitial liquid layer was observed on more than half the peeling length, the regime was considered "adhesive" (represented by full symbols on the adhesion energy graphs). In this case, peeling led to a very visible lifting of the tissues at the detachment front.

4. Characterization of liver hydration and fluid transport

4.1- Measurement of liver water fraction

To evaluate the quantity of water present in the tissues, small liver samples (2-4 cm^3) were dried at 40°C under vacuum until stabilization of their mass (recorded variation below 5 mg). The water weight fraction H was then calculated by the following formula:

$$H = \frac{m_i - m_{dry}}{m_i} \quad \text{(S3)}$$

where m_i is the initial sample mass (hydrated mass) and m_{dry} the sample mass after drying.

The liver samples used for these measurements were cut out from the same liver regions where peeling experiments were performed, and their initial mass was taken at the same time as

the deposition of the hydrogel ribbons on tested tissues so as to reliably replicate hydration conditions found in the tested tissues.

4.2- Swelling experiments

4.2.1 Liver rehydration by swelling

Drained liver parenchyma samples were rehydrated by immersion in physiological serum (NaCl, 9 g/L) at room temperature. For that, samples of different geometry (rectangular or cylindrical section) were rehydrated. Prior to immersion, the volume V, the surface A and the initial mass m_i of each sample was measured. After a certain immersion time, the samples were removed from the serum and precociously shaken to remove excess of superficial liquid after which the swollen mass m_s was measured. The swollen sample was subsequently dried after the method detailed in section 4.1 above to yield the dry extract mass, m_{dry}.

For parenchyma surfaces, the superficial water weight fraction H of rehydrated samples was obtained by considering that the mass of serum gained during immersion is only contained in a superficial tissue layer having a depth b = 0.9 mm, corresponding to half the characteristic size of one lobule. It is thus given by:

$$H = 1 - \left[\frac{1}{1-H_0} + \frac{\Delta m}{m_{dry}}\left(\frac{V}{Ab}\right)\right]^{-1} \quad \text{(S4)}$$

where $H_0 = (m_i - m_{dry})/m_i$ is the water content of the liver sample prior to immersion and $\Delta m = (m_s - m_i)$ is the water uptake after immersion.

4.2.2 Swelling kinetics of PEG on tissues and water reservoir

To follow the swelling kinetics of PEG gels on liver tissues, samples of PEG film (1 cm^2) were deposited on the capsule and parenchyma of a freshly dissected liver (H = 77.9 wt.%) and weighted after different contact times. During the experiment, the liver substrates and the PEG samples were entirely covered by a thin plastic film to avoid water evaporation. Contact time was

varied from 1 to 300 min at room temperature. In a control experiment**,** samples of PEG film (1 cm^2) were deposited on a metal grid floating on a water reservoir and were weighted after different contact times. In that case also, the upper surface of PEG samples was covered by a thin plastic film to avoid water evaporation.

4.3- Optical microscopy.

To study the permeability of the different liver tissue surfaces (parenchyma and capsule), small liver samples were immersed in physiological serum (NaCl, 9g/L) containing 0.1 g/L of small fluorescent solute (sodium Fluorescein, Stokes radius of 0.45 nm as used in similar study) (8). After different immersion times, the samples were taken out of the serum, cut, placed on a DMi8 Video microscope (Leica Microsystems) and imaged with a GFB filter (Excitation wavelength: 470/40 nm - Dichroic mirror: 495 nm – Emission wavelength 525/50 nm).

Final images presented in **Fig. 2C** and **D** are composites of the GFB filtered fluorescent signal and the bright field images with a 30% linear contrast stretch. Isointensity lines were drawn from fluorescence micrographs as the perimeter of the fluorescent signal when the threshold was set to 50% of the maximum intensity.

4.4- Scanning electron microscopy.

The surface state of PEG membranes was characterized by scanning electron microscopy (SEM) on a FEI Nova NanoSEM 450 apparatus operating at an accelerating voltage of 2 kV. Observations were performed on dry hydrogels (Q = 1). Before SEM imaging, specimens were coated with a 2 nm layer of gold/palladium to make the coating conductive.

5. Modeling of fluid transport in liver tissues

5.1- Capillary transport in liver parenchyma

Within the liver parenchyma the blood and bile flow in very small vessels and interstices having a characteristic size of a few microns. *Ex vivo*, once the liver is cut and the parenchyma surface is exposed, the free liquid contained in the lobules rises to the interface through these small vessels. This capillary rise can be described by the Lucas and Washburn law (9-11):

$$h(t) = \left(\frac{\gamma R \cos\theta}{2\eta} \right)^{1/2} t^{1/2} \qquad \text{(S5)}$$

where γ is the surface tension of the liquid, R is the radius of the capillary tube, θ is the contact angle and η is the liquid viscosity. The values of these parameters for liver parenchyma can be assessed by considering blood rising into hydrophilic pores ($\theta \sim 0°$) and selecting commonly used values for the sinusoids radius (8 µm) (12) , the blood viscosity (η = 0.0035 N.s/m²) (13) and the blood surface tension (γ = 55.9 mN/m) (14).

As a result, the time t^* it takes for interstitial fluid to rise at the exposed parenchyma surface and form a layer of thickness h^* is given by:

$$t^* = \left(\frac{h^*}{\Phi} \right)^2 \left(\frac{2\eta}{\gamma R \cos\theta} \right) \qquad \text{(S6)}$$

where Φ is the parenchyma porosity of the order of Φ = 0.3 (11-13). These values give t^* = 0.02 ms for the characteristic time to wet the parenchyma surface with a fluid layer of thickness h^* = 10µm.

5.2- Volume of free liquid available at the surface of liver parenchyma (v_{free})

The volume of a liver lobule V_{lobule} can be decomposed into a tissue part V_{tissue} composed of cells and extracellular matrix and a fluid part V_{fluid} composed of blood and bile contained in the lobule porosities, as follows:

$$V_{lobule} = V_{tissue} + V_{fluid} \tag{S7}$$

We define the characteristic lobule size l as $V_{lobule} \equiv l^3$, and introduce the porosity of the lobules, Φ, defined as the ratio of pore volume (filled with fluid) to the total lobule volume. This gives:

$$V_{fluid} = \Phi\ l^3 \qquad \text{and} \qquad V_{tissue} = (1-\Phi)\ l^3 \tag{S8a,b}$$

We make the two following assumptions:

(A1) The mass of dry extract mostly corresponds to the matter contained in the tissue part. As a result, it should be conserved independently of the hydration of the lobules, which writes:

$$(1-H)\ l^3 = (1-H_0)\ {l_0}^3 \tag{S9}$$

where H is the water content of the tissue and "0" subscript corresponds to a reference state like the state in physiological conditions. For the sake of convenience, density of all components is taken equal to 1 and H is here expressed as a volume fraction instead of a weight fraction.

(A2) As long as there is free fluid in the lobule porosities, the tissue part (cells and extracellular matrix) is assumed to be swollen to equilibrium. Therefore, the volume of the tissue part is conserved, which writes:

$$V_{tissue} = V_{tissue_0} = (1-\Phi_0)\ {l_0}^3 \tag{S10}$$

where "0" subscript corresponds to a reference state like the state in physiological conditions.

Substituting equations (S8b), (S9) and (S10) in equation (S7), the volume of free fluid contained in the lobule of a given piece of *ex vivo* liver parenchyma with water content *H* expresses as:

$$\begin{aligned} V_{fluid} &= V_{lobule} - V_{tissue} \\ &= V_{lobule} - V_{tissue_0} \\ &= l^3 - (1-\Phi_0){l_0}^3 \\ &= \left[1-(1-\Phi_0)\frac{1-H}{1-H_0}\right] l^3 \end{aligned} \tag{S11}$$

where H_0 and Φ_0 are the water content and the porosity of the lobules in a reference state (*e.g.* physiological conditions).

The volume per unit area, v_{free}, of free liquid available at the surface of *ex vivo* liver parenchyma corresponds to the fluid contained in the first layer of superficial lobules. Considering that superficial lobules are on average cut in half, v_{free} is given by:

$$v_{free} = \frac{1}{2}\frac{V_{fluid}}{l^2} \tag{S12}$$

Substituting (S9) and (S11) in (S12) gives:

$$v_{free,\ parenchyma} = \frac{l_0}{2}\left[1-(1-\Phi_0)\left(\frac{1-H}{1-H_0}\right)\right]\left(\frac{1-H_0}{1-H}\right)^{1/3} \tag{S13}$$

In the previously detailed calculation, Φ_0, the porosity fraction in lobular tissues, is taken equal to 0.3 corresponding to volume fraction typically occupied by blood in mammalian livers in physiological conditions (15-17). Similar values of Φ_0 were successfully used for mathematical simulation of liver tissues (18). The lobule characteristic size, l_0, is taken equal to 1.75±0.10 mm in the case of adult pork specimen (drained liver) and to 1.28±0.10 for 3 month old specimen (fresh liver) (19). H_0, the physiological water weight fraction in liver tissues, is taken equal to the average water weight fraction measured in the 3 most hydrated freshly dissected livers (H_0 = 79%) being in the closest state to physiological conditions.

6. *In vivo* adhesion measurements

6.1- Surgical protocol

A total of 2 healthy, one-year-old, Pré-Alpes pig (Sus scrofa domesticus) weighing between 60 and 70 kg were obtained from a licensed vendor (Lebeau Christian, Neuve Maison France). The pig model was selected as the experimental species because of its similarity to humans when monitoring and measuring physiological responses during the procedure.

These pigs were cared for in accordance with the guidelines published by the European Committee for "Care and Use of Laboratory Animals" (Directive 2010/63/EU and the European Convention ETS 123). All procedures were performed in compliance with legislation concerning animal experimentation and approved by the Ethics Committee on Animal Research of ANSES/ENVA/UPEC (C2EA–16, referral number 18-029, 2018030517071534 (# 13915)).

Food was withheld throughout the day and overnight prior to surgery. General anaesthesia was induced with intramuscular injection of xylazine (1.5 mg/kg), ketamine (15 mg/kg) followed by intravenous injection of propofol (4 mg/kg titrated to effect). After orotracheal intubation, anaesthesia was maintained using isoflurane in 02. Analgesia was performed by intravenous injection of morphine chlorhydrate (0.3 mg/kg, redosing to effect).

Animals were ventilated and vital signs (temperature, heart rate, respiration rate, peripheral capillary oxygen saturation, capnography, indirect blood pressure) were monitored and Lactated Ringer's solution was administered intravenously throughout the procedure.

Each pig underwent a ventral midline laparotomy using standard surgical techniques. Briefly, the midline laparotomy was performed from the xiphoid process to the umbilicus. Self-retaining retractors and wetted laparotomy sponges were placed on the abdominal muscular

edges. The liver was exposed and left medial, right medial, and left lateral lobes were isolated and wrapped with moist laparotomy sponges.

The appropriate tested materials were applied on liver capsule to the designated liver lobe and held by gentle digital pressure for 30 seconds. Sites were chosen 1–2 cm apart, to prevent cross-contamination of sites.

After completion of surgical procedures and while under anaesthesia, animals were euthanized by intravenous injection of a sodium pentobarbital-based solution, consistent with the recommendations of the American Veterinary Medical Association (AVMA) Panel on Euthanasia (Leary S et al. AVMA Guidelines for the euthanasia of animals, 2013 edn. https://www.avma.org/KB/Policies/Documents/euthanasia.pdf, American Veterinary Medical Association, Schaumburg, IL).

6.2- Adhesion measurements by tack

For *in vivo* experiments, thin PEG films (0.5 mm thickness) were molded around sterile gauze pads so as to reduce deformation upon water uptake. The absorption rate of those films was comparable to that of PEG films without the embedded textile in the time range of interest (10 min) (see **Fig. S14**).

To measure adhesion *in vivo*, small discs (diameter of 16 mm) were cut from PEG films and ORC meshes. A small metal nut attached to a thin nylon thread loop was glued on the center of the disc. These discs were deposited on the liver capsule by the surgeon and maintained on the tissues under manual pressure for 30 seconds. After a certain time of contact, the discs were detached by pulling on the nylon thread loop.

Control experiments were first performed *in vitro* using a tensile test apparatus (All Around, Zwick) equipped with a 10 N load cell as depicted in **Fig. S15A**. Measurements were performed at a pulling speed of 1mm/s, as shown in **Fig. S15B** for a PEG hydrogel disk. Force-

displacement curves during pulling-off were recorded and allowed for the determination of the tack force, *i.e.* the maximum force (F_{max}) reached during this detachment process, as shown in **Fig. S15C**.

In vivo measurements were performed using a portable dynamometer (FK10 dynamometer from Sauter with a 5 mN resolution). Pulling was applied manually by the same operator in a direction perpendicular to the tissue surface at an approximate speed of 100 mm/s, as shown in **Fig. S16**. The dynamometer allowed to record the maximum force (F_{max}) reached during this detachment process.

7. Statistical analysis

Statistical analysis was carried out on adhesion energies obtained during different peeling regimes (lubricated and adhesive – **Fig. 1F**), hydration levels in different liver tissues (drained and fresh livers – **Fig. S5B**), and adhesion strength obtained *in vivo* with the different gel (PEG and ORC- **Fig. 6G**). Shapiro Wilk test was performed to determine if both populations follow a normal distribution. When normality was verified, raw data were analyzed using an unpaired t-test (**Fig. 1** and **Fig. 6**). On the contrary, data were analyzed using a Mann Whitney test (**Fig. S5**). Statistical significance was accepted at the level of $p < 0.05$.

SI Figures

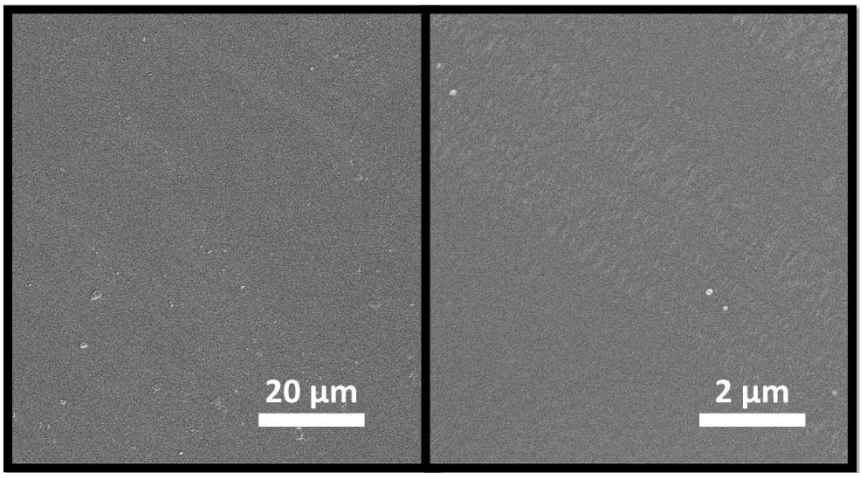

Fig. S1: SEM images of the surface of as-prepared dry PEG hydrogel films.

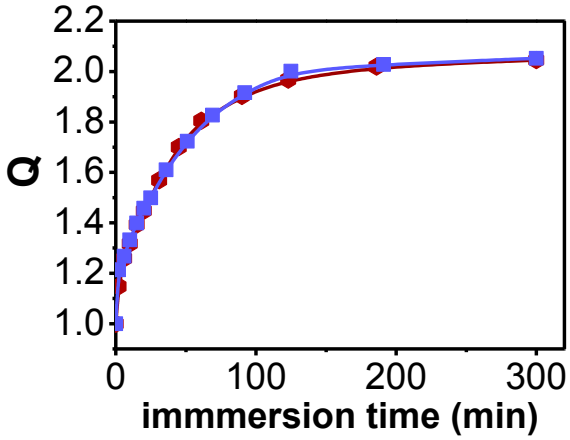

Fig. S2: Swelling ratio of studied 1mm-thick pure PEG films (blue squares) and PEG films modified with RGD (brown hexagons) as a function of immersion time in water.

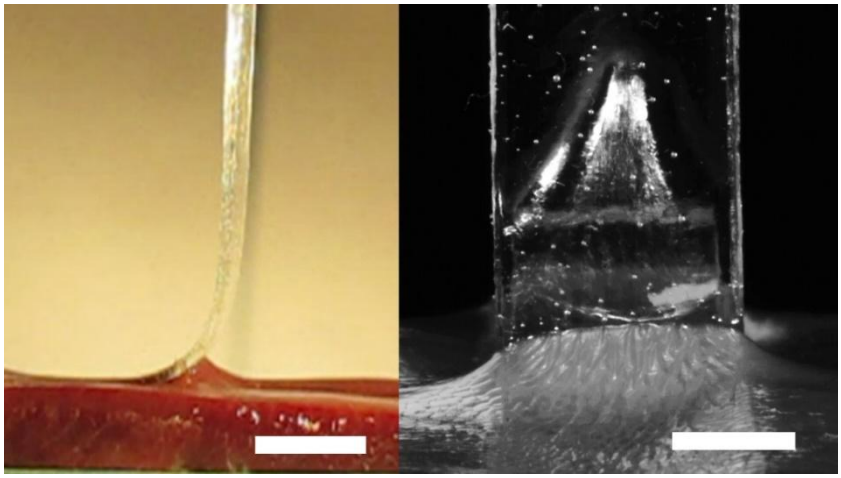

Fig. S3: Side and front views of a peeling experiment performed with a PEG ribbon on freshly dissected liver capsule (Q = 1, Δt = 5 min). A significant tissue deformation is visible. Scale bar: 5 mm.

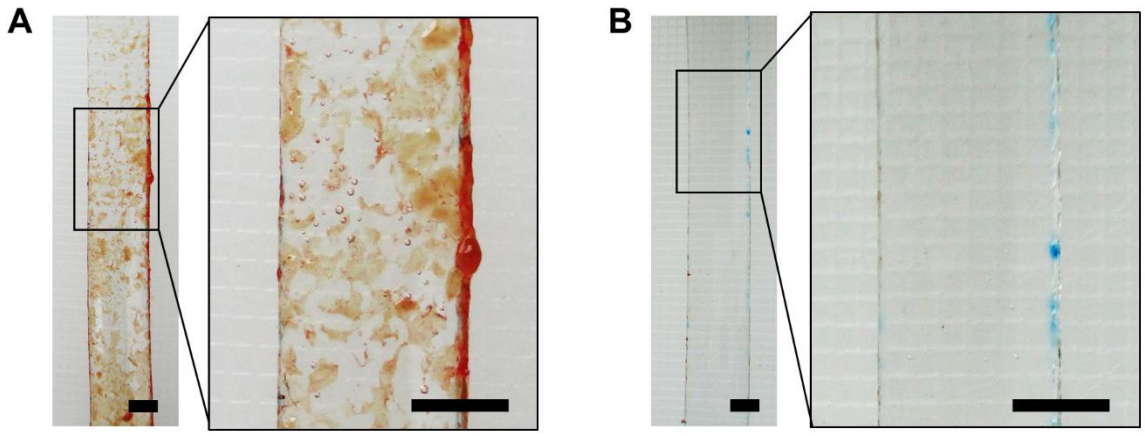

Fig. S4: Photographs of PEG ribbons after peeling exhibiting adhesive regime on fresh liver parenchyma (A) and fresh liver capsule (B). Peeling conditions are Q = 1 and Δt = 5 min. For peeling on the parenchyma (A), tissue deposition is visible on the ribbon. Scale bar: 5 mm.

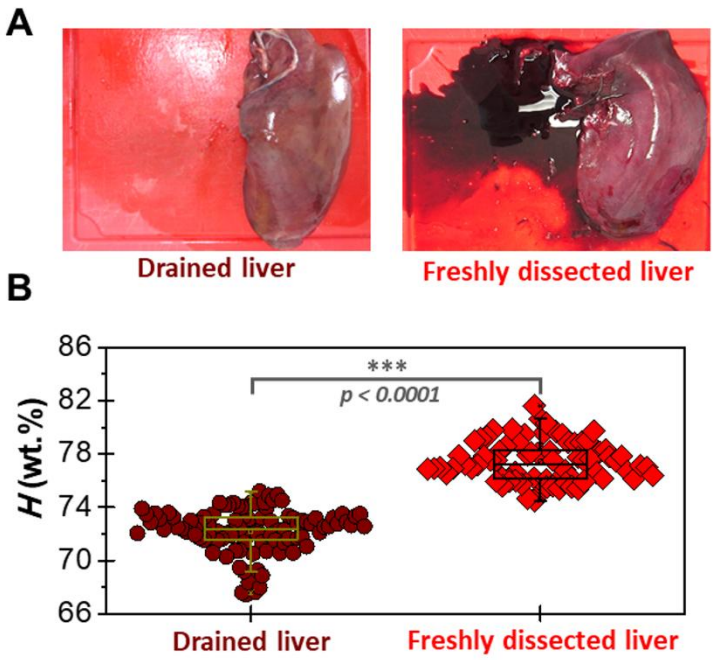

Fig. S5: Hydration of freshly dissected and drained livers. (A) Photographs of a cut lateral lobe from a drained and a freshly dissected liver. (B) Water content in drained and freshly dissected livers. Each point corresponds to one tissue sample taken from several drained livers (N = 16) and freshly dissected livers (N=13).

.

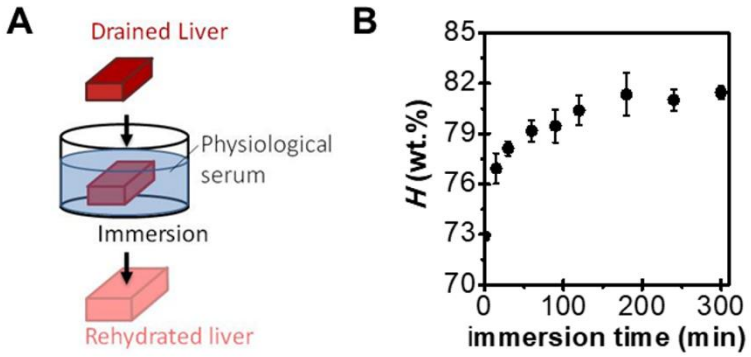

Fig. S6: Rehydration of drained livers. (A) Schematic representation of the rehydration protocol by immersion in physiological serum. (B) Evolution of water fraction *H* in superficial tissues of drained liver parenchyma as a function of immersion time.

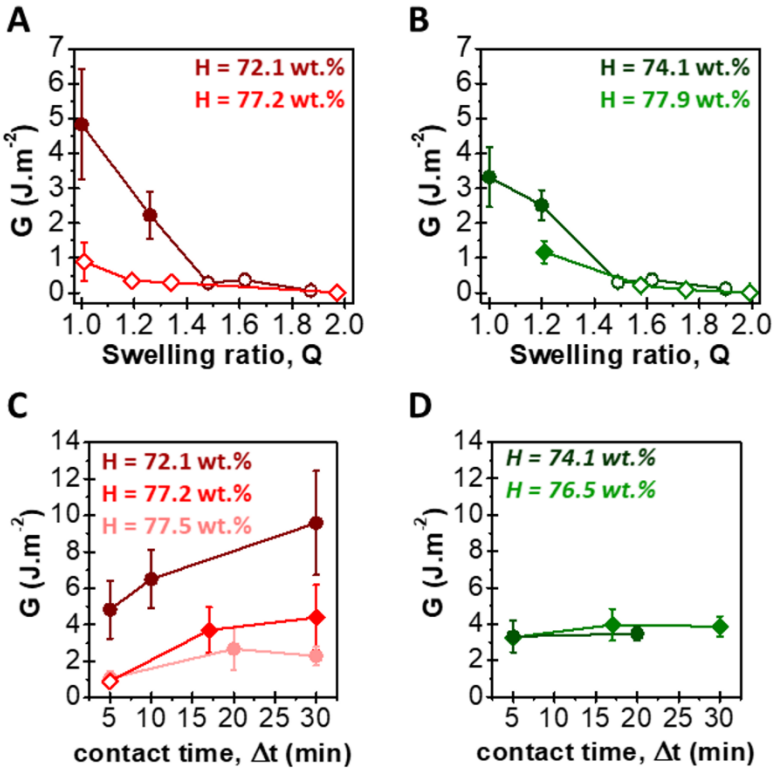

Fig. S7: (A-B) Adhesion energy as a function of the initial swelling ratio of PEG ribbons on the liver parenchyma (A) and capsule (B). Contact time is 5 min. For the parenchyma, drained (brown circles) and freshly dissected livers (red diamonds) were tested. For the capsule, drained (dark green circles) and freshly dissected livers (green diamonds) were tested. (C-D) Adhesion energy as a function of contact time on the liver parenchyma (C) and capsule (D). PEG ribbons were deposited in a dry state (Q = 1). For the parenchyma, drained (brown circles), rehydrated (pink circles) and freshly dissected livers (red diamonds) were tested. For the capsule, drained (dark green circles) and freshly dissected livers (green diamonds) were tested. Full and open symbols correspond to adhesive and lubricated regimes, respectively. Water fraction of substrate tissues are mentioned for each figure with corresponding colors.

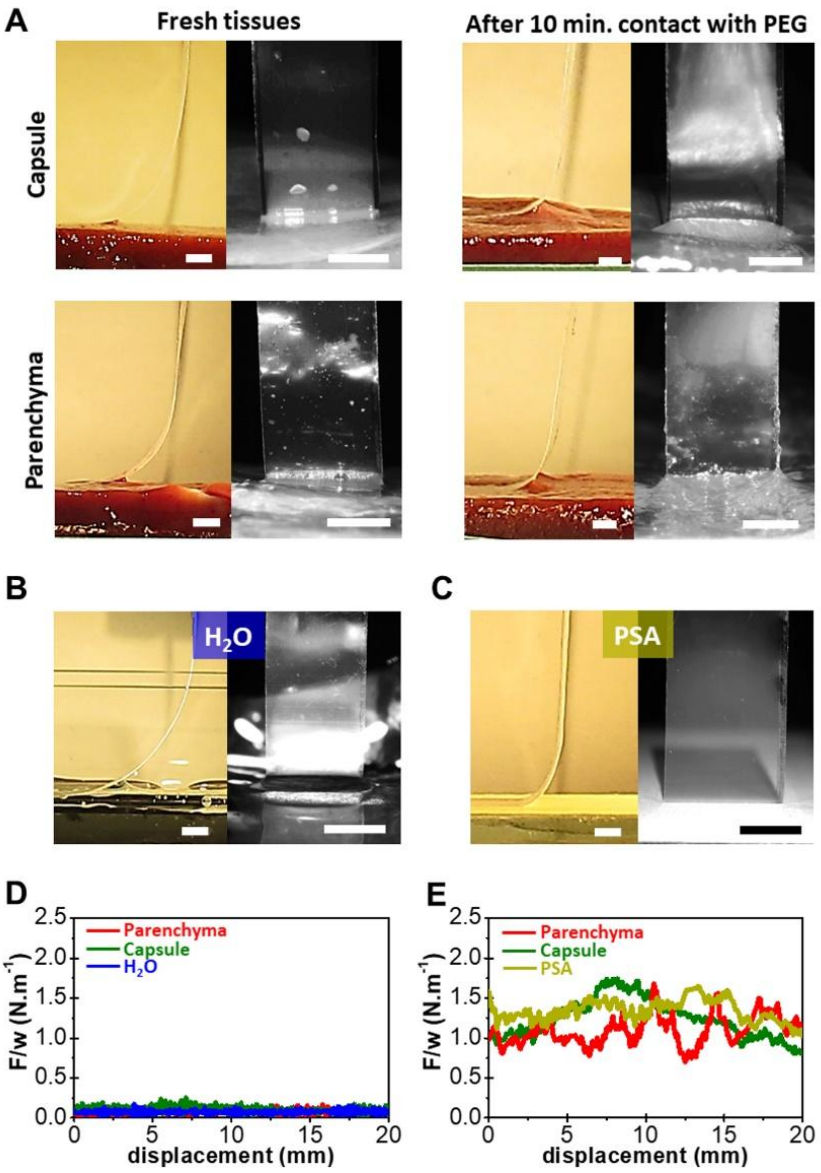

Fig. S8: Adhesion of polyethylene ribbons on freshly dissected liver capsule and parenchyma before and after 10 min contact with a PEG hydrogel film (Q = 1). (A) Side and front views of the peeling experiments. Experiments are compared to peeling of the same polyethylene ribbons from a water surface (B) and from a pressure sensitive adhesive (PSA) (C). Contact time is 5 min for all experiments. Scale bar: 5 mm. (D) Corresponding peeling curves for polyethylene ribbons on freshly dissected liver capsule (green) and parenchyma (red). They are compared to the peeling curve obtained on a water surface (blue). (E) Corresponding peeling curves for polyethylene ribbons on tissues previously put in contact with a dry PEG film for 10 min: capsule (green), parenchyma (red). They are compared to the peeling curve obtained on a PSA (yellow).

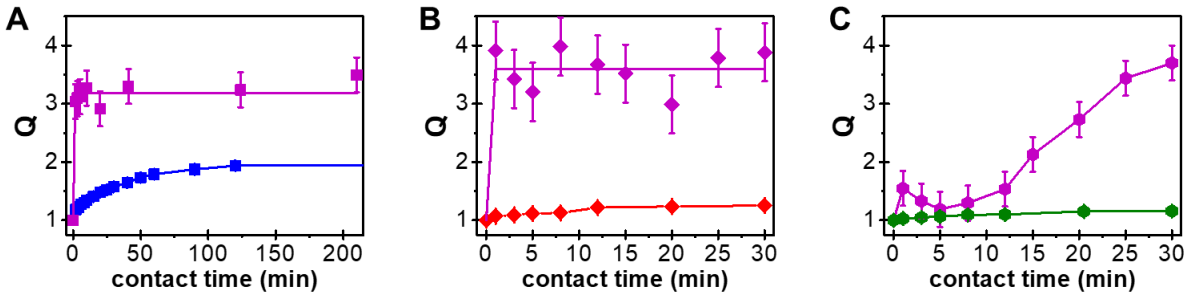

Fig. S9: Swelling behavior of Oxidized Regenerated Cellulose (ORC) meshes. (A) Swelling of ORC by immersion in water (violet squares) compared to that of PEG films (blue squares). (B) Swelling of ORC by deposition on fresh liver parenchyma with H = 77.9 wt.% (violet diamonds) compared to that of PEG films in the same conditions (red diamonds). (C) Swelling of ORC by deposition on fresh liver capsule (violet hexagons) compared to that of PEG films in the same conditions (green hexagons).

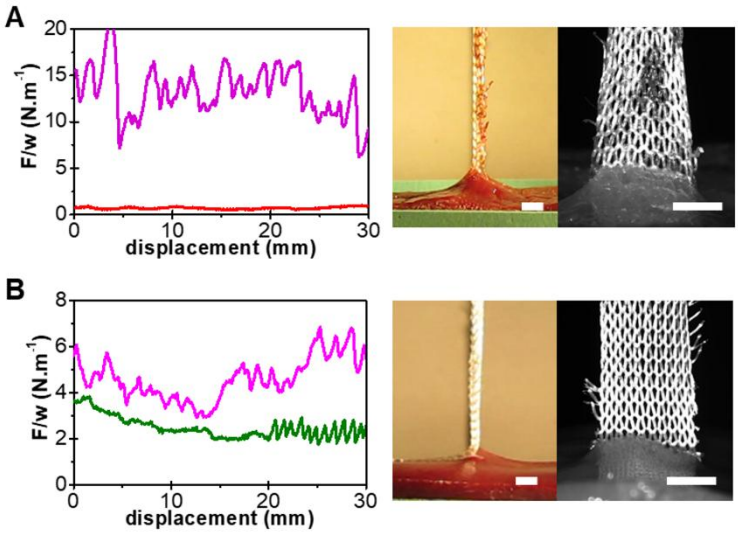

Fig. S10: *Ex vivo* adhesion of dry ORC meshes. (A) Peeling force recorded for ORC meshes (violet curve) and a PEG ribbon (red curve) on liver parenchyma (H = 77.4 ± 0.2 wt.%). Side and front views of the corresponding peeling of ORC meshes from liver parenchyma. (B) Peeling force recorded for ORC meshes (violet curve) and a PEG ribbon (green curve) on liver capsule. Side and front views of the corresponding peeling of ORC meshes on liver capsule. (scale bar: 5 mm).

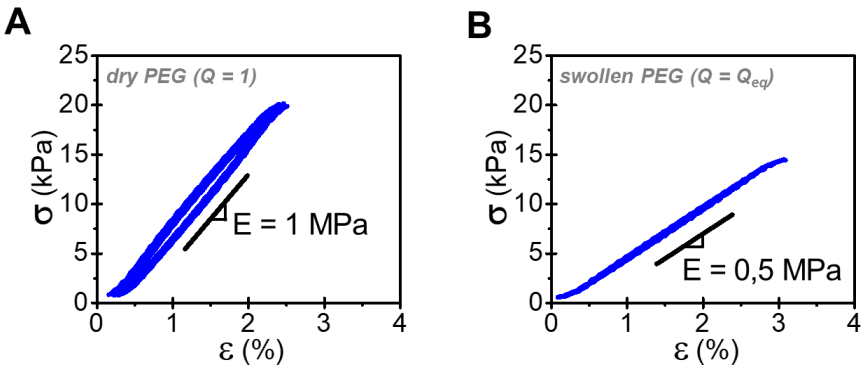

Fig. S11: Tensile stress-strain curves of PEG films in dry state (A) and swollen to equilibrium in water (B) starring the Young's modulus for both systems.

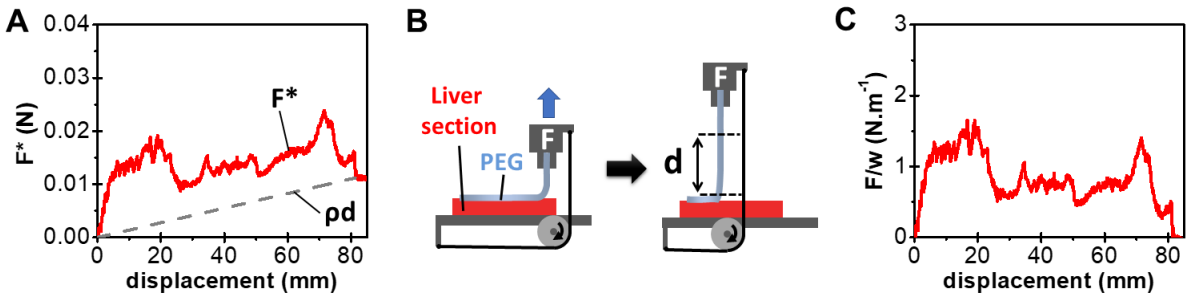

Fig. S12: (A) Force as measured by the force cell as a function of displacement during a peeling experiment on liver. Dash line shows the calculated weight of the lifted ribbon, which increases as peeling proceeds. (B) Schematic representation showing the length of lifted ribbon *d*. (C) Peeling force corrected from the weight of the lifted ribbon and normalized by the ribbon width as a function of displacement.

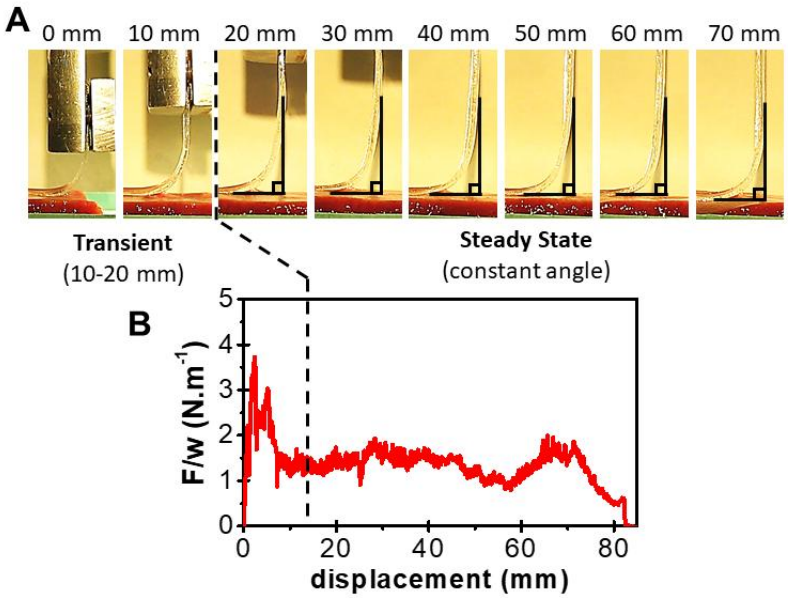

Fig. S13: Determination of the peeling steady state. (A) Snapshots of the peeling of a PEG ribbon on a fresh liver capsule from a side view. (B) Peeling force recorded during the corresponding experiment. The steady state peeling at a constant angle equal to 90° is here obtained after about 15 mm of displacement.

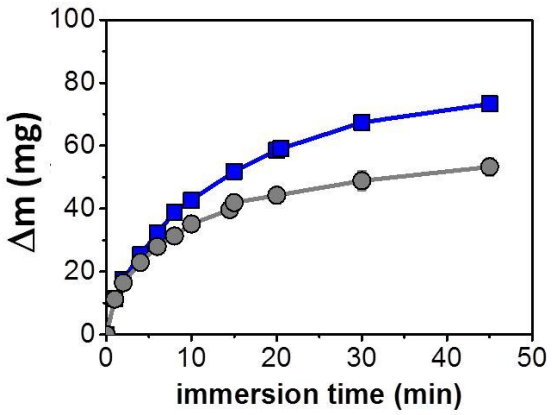

Fig. S14: Water uptake of PEG membranes (blue squares) and PEG membranes reinforced with sterile gauze pad (grey circles) when immersed in water. Both membranes have a thickness of 0.5 mm.

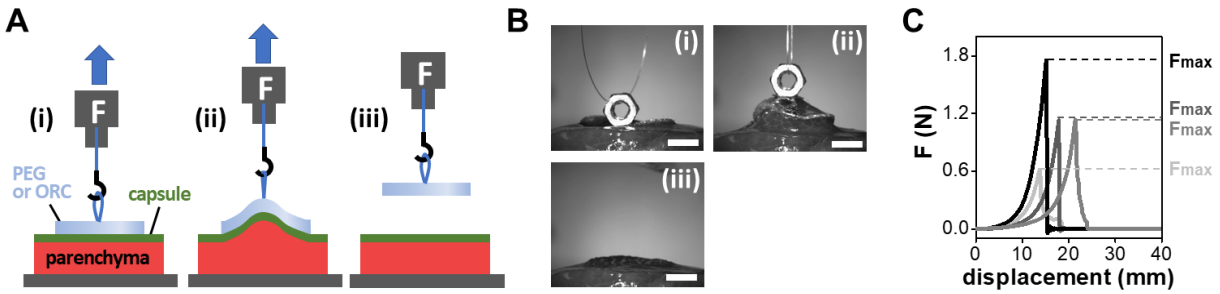

Fig. S15: *Ex vivo* tack-like adhesion measurement performed in an electromechanical testing apparatus. (A) Schematic drawings of the tack experiment in initial state (i), during pulling (ii) and after detachment of the hydrogel disk from the liver capsule *ex vivo* (iii). (B) Snapshots taken during the pulling of a PEG disk from a fresh liver capsule *ex vivo* (Δt = 10 min; pulling speed = 1 mm/sec; scale bar: 5 mm). (C) Force curves recorded during the pulling of PEG disks from fresh liver capsule *ex vivo*. The maximum force measured, F_{max}, is displayed for each curve.

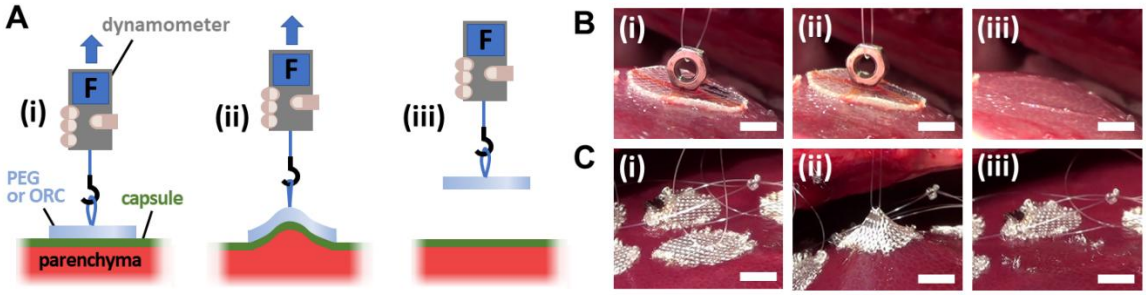

Fig. S16: *In vivo* tack-like adhesion measurement. (A) Schematic drawings of the tack experiment in initial state (i), during manual pulling (ii) and after detachment of the hydrogel disk from the liver capsule *in vivo* (iii). (B-C) Snapshots of tack experiments performed *in vivo* on porcine liver capsule with a PEG membrane (B) and an ORC mesh (C) (Δt = 10 min; scale bar: 5 mm).

SI Video captions

Video S1: Side and front video of the peeling of a PEG ribbon on fresh liver parenchyma exhibiting a lubricated behavior. (Accelerated 10 times; scale bar: 5 mm)

Video S2: Side and front video of the peeling of a PEG ribbon on fresh liver parenchyma exhibiting an adhesive behavior. (Accelerated 10 times; scale bar: 5 mm)

Video S3: Side and front video of the peeling of a PEG ribbon on fresh liver capsule. (Accelerated 10 times; scale bar: 5 mm)

Video S4: Front videos of the peeling of a polyethylene ribbon on fresh liver capsule before (left hand side) and after (right hand side) dehydration by a 10 minutes contact with a dry PEG ribbon. (Accelerated 10 times; scale bar: 5 mm)

Video S5: Front videos of the peeling of a polyethylene ribbon on fresh liver parenchyma before (left hand side) and after (right hand side) dehydration by a 10 minutes contact with a dry PEG ribbon. (Accelerated 10 times; scale bar: 5 mm)

Video S6: Video of an *ex vivo* tack-like experiment displaying the detachment of a circular film of dry PEG from fresh liver capsule after 10 minutes of contact. (Accelerated 10 times; scale bar: 5 mm)

Video S7: Video of an *ex vivo* tack-like experiment displaying the detachment of a circular patch of dry ORC mesh from fresh liver capsule after 10 minutes of contact. (Accelerated 10 times; scale bar: 5 mm)

Video S8: Video of a tack-like experiment displaying the detachment of a dry ORC circular mesh from liver capsule *in vivo* after 10 minutes of contact. The entire hepatic lobe is lifted upwards during the experiment. (Accelerated 2 times; scale bar: 10 mm)

SI References

1. Strange ED, Dahms MP, Benedict RC, & Woychik JH (1985) Changes in connective tissue histology in freeze-thaw cycled and refrigerated pork liver. *Journal of Food Science* 50(5):1484-1485.
2. Liu SQ, *et al.* (2010) Injectable biodegradable poly(ethylene glycol)/RGD peptide hybrid hydrogels for in vitro chondrogenesis of human mesenchymal stem cells. *Macromolecular Rapid Communications* 31(13):1148-1154.
3. Kudva AK, Luyten FP, & Patterson J (2018) RGD-functionalized polyethylene glycol hydrogels support proliferation and in vitro chondrogenesis of human periosteum-derived cells. *J. Biomed. Mater. Res. Part A* 106(1):33-42.
4. Hern DL & Hubbell JA (1998) Incorporation of adhesion peptides into nonadhesive hydrogels useful for tissue resurfacing. *J Biomed Mater Res* 39(2):266-276.
5. Rebizant V, Abetz V, Tournilhac F, Court F, & Leibler L (2003) Reactive tetrablock copolymers containing glycidyl methacrylate. Synthesis and morphology control in epoxy−amine networks. *Macromolecules* 36(26):9889-9896.
6. Kendall K (1975) Thin-film peeling - elastic term. *J. Phys. D-Appl. Phys.* 8(13):1449-1452.
7. Peng ZL & Chen SH (2015) Effect of bending stiffness on the peeling behavior of an elastic thin film on a rigid substrate. *Phys. Rev. E* 91(4).
8. Fu BM & Shen S (2003) Structural mechanisms of acute VEGF effect on microvessel permeability. *American journal of physiology. Heart and circulatory physiology* 284(6):H2124-2135.
9. Chen J, Park H, & Park K (1999) Synthesis of superporous hydrogels: Hydrogels with fast swelling and superabsorbent properties. *J. Biomed. Mater. Res.* 44(1):53-62.
10. Lucas R (1918) Ueber das zeitgesetz des kapillaren aufstiegs von flüssigkeiten. *Kolloid-Zeitschrift* 23(1):15-22.
11. Washburn EW (1921) The dynamics of capillary flow. *Physical Review* 17(3):273-283.
12. MacPhee PJ, Schmidt EE, & Groom AC (1995) Intermittence of blood flow in liver sinusoids, studied by high-resolution in vivo microscopy. *The American journal of physiology* 269(5 Pt 1):G692-698.
13. Lowe GD, Lee AJ, Rumley A, Price JF, & Fowkes FG (1997) Blood viscosity and risk of cardiovascular events: the Edinburgh Artery Study. *British journal of haematology* 96(1):168-173.
14. Hrncir E & Rosina J (1997) Surface tension of blood. *Physiological research* 46(4):319-321.
15. Rothe CF (1993) Regulation of hepatic vascular capacitance. *Veins: Their Functional Role in the Circulation*, eds Hirakawa S, Rothe CF, Shoukas AA, & Tyberg JV (Springer Japan, Tokyo), pp 90-97.
16. Schafer J, D'Almeida MS, Weisman H, & Lautt WW (1993) Hepatic blood volume responses and compliance in cats with long-term bile duct ligation. *Hepatology* 18(4):969-977.

17. Greenway CV & Lautt WW (2010) Hepatic circulation. *Comprehensive Physiology*, (John Wiley & Sons, Inc.).
18. White D, Coombe D, Rezania V, & Tuszynski J (2016) Building a 3D virtual liver: methods for simulating blood flow and hepatic clearance on 3D structures. *PLoS ONE* 11(9).
19. White EG (1939) Some observations on the liver of the pig: the hepatic lobule and liver cell during post-natal growth. *Journal of Anatomy* 73(Pt 3):365-386.361.